

Phonon-assisted tunneling in interacting suspended single wall carbon nanotubes

Wataru Izumida^{1,2} and Milena Grifoni³

¹Department of Physics, Tohoku University, Sendai 980-8578, Japan

²Kavli Institute of Nanoscience, Delft University of Technology, Lorentzweg 1, 2628 CJ Delft, The Netherlands

³Department of Physics, University of Regensburg, D-93040 Regensburg, Germany

E-mail: izumida@cmpt.phys.tohoku.ac.jp

Abstract. Transport in suspended metallic single wall carbon nanotubes in the presence of strong electron-electron interaction is investigated. We consider a tube of finite length and discuss the effects of the coupling of the electrons to the deformation potential associated to the acoustic stretching and breathing modes. Treating the interacting electrons within the framework of the Luttinger liquid model, the low-energy spectrum of the coupled electron-phonon system is evaluated. The discreteness of the spectrum is reflected in the differential conductance which, as a function of the applied bias voltage, exhibits three distinct families of peaks. The height of the phonon-assisted peaks is very sensitive to the parameters. The phonon peaks are best observed when the system is close to the Wentzel-Bardeen singularity.

1. Introduction

Carbon nanotubes are new prototypical candidates for one-dimensional nanoconductors. As such, electron transport through such macromolecules has been investigated extensively. Single wall carbon nanotubes (SWNTs) behave as metallic ($n - m = 3l$, l is an integer) or semiconducting conductors ($n - m \neq 3l$) depending on their wrapping vector, $(n, m) \equiv n\vec{a}_1 + m\vec{a}_2$, where \vec{a}_1 , \vec{a}_2 are the graphene primitive lattice vectors. [1, 2, 3]. Moreover, Coulomb blockade phenomena, the Kondo effect, and Tomonaga-Luttinger liquid properties have been experimentally demonstrated [4, 5, 6, 7, 8]. Such measurements confirm the relevance of electron correlations effects in SWNTs at low energies as predicted in earlier theoretical studies [9, 10, 11]. Recently, suspended nanotubes have been fabricated, and the transport properties have been measured by several groups [12, 13, 14, 15, 16]. Since the suspended nanotube is free from the substrate, it is expected that it can easily vibrate [16, 17]. At the same time, some theoretical works have started to investigate the effects of the mechanical motion on the electronic transport properties of interacting SWNTs [18, 19, 20, 21]. While Ref. [19, 21] focus on Coulomb blockade phenomena, the SWNT is treated as a Tomonaga-Luttinger liquid [22] with periodic boundary conditions (valid for very long nanotubes) in Ref. [18, 20]. However, typical SWNT lengths are of the order of sub-micron to micrometers, yielding a mean level spacing for the electronic energy levels in the meV energy range. This discreteness of the energy levels can be clearly seen in low temperature measurements, e.g. by measuring the excitation spectrum of a SWNT quantum dot [23]. In finite length SWNTs, the quantized nature of the vibrational modes of a SWNT should be considered as well at low enough energies.

In this paper, we investigate the effects of the mechanical vibrations on the electronic properties of a doubly clamped SWNT of finite length within a full quantum mechanical treatment of the low energy excitations. Even if the metallic condition $n - m = 3l$ is satisfied, small energy gaps $\sim 10\text{meV}$ appear due to curvature effects. The armchair nanotubes ($n = m$), however, still stay metallic because of their high symmetry [24]. Therefore we consider the armchair SWNTs in this paper. The interacting electrons in the nanotubes are considered within the standard bosonization framework of the Tomonaga-Luttinger liquid model with open boundary conditions [25, 26], where the electronic excitations (charged and neutral plasmons) have bosonic character. The low energy vibrations of the nanotube can be described in terms of acoustic phonons, associated to the longitudinal stretching mode and to the transverse twisting and breathing modes [27]. The coupling between electron and phonons is described in terms of the deformation potential caused by the acoustic modes. In our model this yields a bilinear bosonic coupling between phonons and plasmons. In Ref. [20], the acoustic modes have been treated within a continuous elastic model, and have been integrated out in order to obtain a phonon-mediated retarded electron-electron interaction. It was shown that while the twisting mode can be neglected at low energies, the effect of the breathing mode and stretching modes should be considered. In particular, retardation

effects of the breathing mode can be neglected, and an effective renormalization of the electron-electron interaction strength is found with possibly attractive interactions. In contrast, retardation effects due to the stretching mode must be retained, so that, due to the combined effects of stretching and breathing modes, the Wentzel-Bardeen singularity, describing a superconducting instability of the electron-phonon system [28], can be reached. In this paper, we consider the case in which electron *as well as* phonon modes are quantized, and look to the energy spectrum of the interacting electron-phonon system. As in Ref. [20], the major effect of the breathing mode is to renormalize the electron-electron interaction strength. On the other hand the electronic as well as the stretching-phonons parameters get renormalized by the mutual interaction, yielding "electron"-like and "stretching-phonons"-like excitations. Such electron-like excited levels appear as large peaks in the differential conductance, while stretching-phonon-like assisted processes appear as small peaks beside the large peaks. The phonon peak height is very sensitive to the system parameters, and it becomes larger and larger when the value of the charged plasmons' velocity is close to the sound velocity, i.e. when the Wentzel-Bardeen instability [28] is approached. Thus, the experimental observation of the phonon peak would be an indication of the strong fluctuation of the superconducting order parameter, which corresponds to the Wentzel-Bardeen singularity, in SWNTs. At temperatures higher than the level spacing, the discreteness of the peaks is washed out. The differential conductance then shows the characteristic Tomonaga-Luttinger power-law dependence on voltage, with exponents modified by the electron-phonon interaction.

2. Low-energy Hamiltonian

To start with, we consider a suspended, doubly clamped metallic SWNT whose fixed ends are at $x = 0$ and $x = L$. We wish to develop a low energy theory for suspended metallic SWNTs, and restrict ourselves to the two lowest linear in k electronic subbands. Moreover, in experiments the nanotubes are typically intrinsically *p*-doped such that the Fermi level is shifted away from half-filling. Long-range Coulomb interaction is dominant in isolated SWNTs, because the electrons are spread out around the circumference of the tube, and the probability of two electrons to be near to each other is of the order $1/N$, where N is the number of atoms on the circumference. The interaction is usually screened on a length determined either by the tube length or by the distance to nearby gates. The Coulomb interaction causes Umklapp, backward and forward scattering processes among the electrons. Away from half-filling Umklapp scattering can be neglected. We also disregard backscattering processes, which is a valid approximation if the tube radius is not too small [11]. The forward scattering processes can be fully included within a Tomonaga-Luttinger (TL) model for SWNTs [9, 10, 11], yielding the TL Hamiltonian

$$H_{\text{el}} = H_N + \sum_j H_j , \quad (1)$$

$$H_j = \frac{v_j}{2} \int_0^L dx \left[g_j \Pi_j^2(x) + \frac{1}{g_j} (\partial_x \phi_j(x))^2 \right], \quad (2)$$

where the index $j = c+, s+, c-, s-$ counts the four excitation sectors for total charge, total spin and relative (with respect to the two electronic subbands) charge and relative spin, respectively. The first term $H_N = \sum_j E_j N_j^2/2$ in Eq. (1) represents the ground state energy. The quantities E_j are the energies for total/relative charge and spin for a given number of electrons $N_{c\pm}$ and given spin $N_{s\pm}$. Specifically, E_{c+} contains the charging and single particle energies and is taken as a free-parameter hereafter, in order to include screening effects of nearby gates. For the remaining modes is $E_j = \varepsilon_0/4$, with $\varepsilon_0 = \hbar v_F \pi / L$ the single particle level spacing. Here we denoted with v_F the Fermi velocity, while L is the SWNT length. For SWNTs the term $\varepsilon_0 \delta N_{c-}$ should be added in H_N , where δ is a small off-set caused by the discrepancy of the discretized energies between the two bands. The gate potential term $-e N_{c+} V_G$ is also added in the Hamiltonian. The second term in Eq. (1) describes the collective bosonic excitations of the one-dimensional interacting electron system. $\Pi_j(x)$ and $\phi_j(x)$ play the role of the momentum and displacement field operators, respectively, and they are conjugate variables of each other, i.e., $[\phi_j(x), \Pi_{j'}(x')] = i\hbar \delta_{jj'} \delta(x - x')$. Due to the interaction, the excitations propagate with renormalized velocity $v_j = v_F/g_j$, where g_j is the interaction parameter for the j -sector. Because the Coulomb interaction describes an interaction among total electronic densities, only the total charge sector is affected while the other sectors are neutral sectors, i.e., $g_{c+} < 1$ and $g_j = 1$ ($j = s+, c-, s-$), respectively. Hereafter we denote $g = g_{c+}$ and we call $j = c+$ the charge sector simply. The interaction parameter is roughly estimated as $g = 1/\sqrt{1 + U/\hbar v_F \pi}$ with $U = 8e^2 \log R_{sc}/R$. Here R_{sc} is a phenomenologically introduced screening scale, long compared with the tube radius R . It can be estimated to be $R_{sc} = \min\{L, d\}$, where $L \simeq 1\mu\text{m}$ is a typical SWNT length, and d is the distance to a possibly present gate electrode. The interaction parameter is estimated to be $g \simeq 0.2$ for $R_{sc} \simeq 1\mu\text{m}$ [10]. The screening caused by a gate electrode nearby the nanotube is typically more effective in screening, which pushes g closer to the non-interacting value, $g = 1$.

We consider next the effects of the vibrations. The relevant phonon modes at low energies are those for which the quantized (due to the periodic boundary conditions in the circumference direction) transverse momentum is zero. There are three modes: stretching, twisting and breathing modes. In terms of the deformation potential, the transverse-acoustic twisting mode does not contribute at first order in the displacement [20], so that it will no longer be considered in the rest of this work. The transverse acoustic breathing mode has a finite frequency ω_B , of the order of $(0.14/\hbar R)\text{meV}\text{\AA}$ in the long wavelength limit. The energy scale is thus larger than that of the low energy electrons in the vicinity of the Fermi energy. However, as we shall discuss later, this mode strongly renormalizes the energy of the charge sector. In the following, we start by explicitly considering the effects of the coupling to the longitudinal stretching mode. We start from a continuum model for the vibrations [27], such that the stretching mode corresponds to the longitudinal acoustic mode of the one-dimensional continuum. At a

second stage of the calculation also the effect of the breathing mode will be discussed. The Hamiltonian for the longitudinal phonons and the electron-phonon interaction are written as

$$H_{\text{L,ph}} = \frac{1}{2} \int_0^L dx \left[\frac{1}{\zeta} P^2(x) + \zeta v_{\text{st}}^2 (\partial_x u(x))^2 \right], \quad (3)$$

$$H_{\text{el-L,ph}} = c \int_0^L dx \rho(x) \partial_x u(x), \quad (4)$$

where ζ is the carbon mass per unit length, v_{st} is the sound velocity of the stretching mode, c is the electron-phonon coupling constant, and $\rho(x) = 2\partial_x \phi_{\text{c+}}(x)/\sqrt{\pi\hbar} + N_{\text{c+}}/L$ is the electron density. $P(x)$ and $u(x)$ are the momentum and displacement field operators, obeying the commutation relation $[u(x), P(x')] = i\hbar\delta(x - x')$.

Before we proceed, let us discuss the relation between the coupling constant c of our one-dimensional model and the three-dimensional nature of the electron-phonon coupling in SWNTs. For a SWNT the electron-phonon interaction is written as [27]

$$H_{\text{el-ph}} = \int_0^{2\pi R} dy \int_0^L dx \rho(x, y) V(x, y), \quad (5)$$

where the y axis is along the circumference, $\rho(x, y)$ is the density of electrons and $V(x, y)$ is the deformation potential. For the stretching phonon mode $V(x, y) = 2c'\partial_x u_x \mu/(B + \mu)$ has no y -dependence. Here u_x is the displacement field, and B , μ and c' are the bulk modulus, shear modulus and deformation potential for a graphene sheet, respectively. Therefore, with $\rho(x) = \int_0^{2\pi R} \rho(x, y) dy$, we have the relation $c = 2c'\mu/(B + \mu)$.

Since we want to investigate transport properties of the coupled electron-phonon system in a tube of finite length L , we employ open boundary conditions for the electrons, $\Pi_j(0) = \Pi_j(L) = 0$, and $\phi_j(L) - \phi_j(0) = 0$ [10, 25, 26]. For the phonon field we have similar boundary conditions, $P(0) = P(L) = 0$, $u(0) = u(L) = 0$. The discreteness of the phonon and electron spectrum in a finite length SWNT is better visualized by expanding each field operator in Fourier series as

$$\phi_j(x) = \sqrt{\frac{\hbar g_j}{L}} \sum_{n \geq 1} \sin(k_n x) \frac{1}{\sqrt{k_n}} (b_{j,n}^\dagger + b_{j,n}), \quad (6)$$

$$\Pi_j(x) = i \sqrt{\frac{\hbar}{g_j L}} \sum_{n \geq 1} \sin(k_n x) \sqrt{k_n} (b_{j,n}^\dagger - b_{j,n}). \quad (7)$$

Here $b_{j,n}$ ($b_{j,n}^\dagger$) are annihilation (creation) operators of the j -sector's bosons, satisfying $[b_{j,n}, b_{j',n'}^\dagger] = \delta_{jj'}\delta_{nn'}$, and $k_n = \pi n/L$ is the wave number. Similar expansions hold for $u(x)$ and $P(x)$:

$$u(x) = \sqrt{\frac{\hbar}{\zeta v_{\text{st}} L}} \sum_{n \geq 1} \sin(k_n x) \frac{1}{\sqrt{k_n}} (a_n^\dagger + a_n), \quad (8)$$

$$P(x) = i \sqrt{\frac{\hbar \zeta v_{\text{st}}}{L}} \sum_{n \geq 1} \sin(k_n x) \sqrt{k_n} (a_n^\dagger - a_n), \quad (9)$$

where a_n (a_n^\dagger) are the annihilation (creation) operators of the phonon mode obeying the commutation relation $[a_n, a_{n'}^\dagger] = \delta_{nn'}$. Using these relations we get

$$H_{\text{el}} = \sum_{j,n \geq 1} \varepsilon_j n b_{j,n}^\dagger b_{j,n} + H_N, \quad (10)$$

$$H_{\text{L,ph}} = \sum_{n \geq 1} \varepsilon_a n a_n^\dagger a_n, \quad (11)$$

$$H_{\text{el-L,ph}} = \sum_{n \geq 1} I n (a_n^\dagger + a_n) (b_{c+,n}^\dagger + b_{c+,n}). \quad (12)$$

Here $\varepsilon_j = \varepsilon_0/g_j$ is the discrete excitation energy for the j -sector, while $\varepsilon_a = \hbar v_{\text{st}} \pi/L$ for the phonons. Finally, $I = c\sqrt{\hbar g/\pi \zeta v_{\text{st}} \pi/L}$ is the electron-phonon coupling. The electron-phonon interaction term (12) reflects the fact that the phonons couple only to the total charge density via the deformation potential. The Hamiltonian $H = H_{\text{el}} + H_{\text{L,ph}} + H_{\text{el-L,ph}}$ is bi-linear in the boson operators characterizing the electronic and phonon excitations, and as such it can be exactly diagonalized with a Bogoliubov transformation (see Appendix). The diagonalized Hamiltonian is,

$$H = \sum_{n \geq 1} E_\beta n \beta_n^\dagger \beta_n + \sum_{n \geq 1} E_\alpha n \alpha_n^\dagger \alpha_n + \sum_{j',n \geq 1} \varepsilon_0 n b_{j' \neq c+,n}^\dagger b_{j',n} + H_N, \quad (13)$$

where $E_{\beta/\alpha}$ comes from the branch of the charge density/phonon, defined by,

$$E_{\beta/\alpha} = \sqrt{\frac{\varepsilon_a^2 + \varepsilon_{c+}^2}{2} \pm \sqrt{\left(\frac{\varepsilon_{c+}^2 - \varepsilon_a^2}{2}\right)^2 + 4I^2 \varepsilon_a \varepsilon_{c+}}}. \quad (14)$$

Here we assumed the relation $\varepsilon_a < \varepsilon_{c+}$, as it holds for carbon nanotubes. The summation j' in Eq. (13) is for the neutral sectors $j' = c-, s+, s-$. We notice that for electron-phonon couplings $I^2 = \varepsilon_a \varepsilon_{c+}/4$ the energy E_α vanishes. For even larger couplings E_α becomes complex which is an unphysical situation. Thus we require that $I^2 \leq \varepsilon_a \varepsilon_{c+}/4$, where the equality sign defines the Wentzel-Bardeen singularity. We notice that also the diagonalized energies have a linear dispersion relation. Hereafter we use the index $\mu = \alpha, \beta, \nu$ for the three kinds of bosonic excitations, and set $E_\nu = \varepsilon_0$.

Let us now also include the effects of the breathing mode. A quantitative estimate of these effects is discussed in [20], where the authors evaluate the effective retarded electronic action obtained upon integrating out the phonon stretching and breathing modes. It turns out that retardation effects can be disregarded for the breathing but not for the stretching mode. Thus the breathing mode yields a renormalization of the velocity associated to the charged plasmon mode as $v_{c+}^* = a_B v_{c+}$, where

$$a_B = \sqrt{1 - \frac{R_B}{R} g^2}, \quad (15)$$

and $R_B \simeq 2.4 \pm 0.9 \text{ \AA}$ [20]. With $v_F = 8 \times 10^5 \text{ m/sec}$, $v_{\text{st}} = 2 \times 10^4 \text{ m/sec}$, and interaction parameter $g = 0.2$ the charge velocity v_{c+}^* becomes *comparable* to the sound velocity v_{st} of the stretching mode if $a_B \simeq 5 \times 10^{-3}$. This cannot occur, not even for the smallest SWNT radii. However, the renormalized charge velocity might become of the order

of the sound velocity v_{st} for realistic nanotube radii for strongly screened interaction (yielding values of g close to one). The breathing mode also yields a renormalization of the electron-electron interaction parameter as $g^* = v_{\text{F}}/v_{\text{c+}}^* = g/a_{\text{B}}$. This results in the increase of the electron-phonon coupling in Eq. (12) with $(I^*)^2 = I^2/a$. In the following, we shall then consider breathing-mode renormalized parameters, with a parameter $a_{\text{B}} = 0.993$ ($g = 0.2$), 0.804 ($g = 1$) as for a realistic (10, 10) tube.

We notice that also Umklapp scattering processes should reduce the charge velocity [29]. This effect would be dominant near half-filling, where a strong coupling with the stretching mode is expected [28]. Moreover, a suppression of the electron-phonon coupling is expected at half-filling [30, 31]. This situation has not been considered in our calculation, since SWNTs are usually away from half-filling [11].

3. Phonon assisted tunneling

With the help of Eq. (13) we can now evaluate the density of states $\rho(\epsilon)$. In particular, we shall focus on the density of states at a nanotube end ρ_{end} , yielding direct information on the differential conductance. The density of states is calculated by expressing the electron field operators in terms of the boson operators [9, 10, 11]. After lengthy but standard calculations, see Appendix, we arrive at the following finite temperature density of states at the end of the nanotube:

$$\rho_{\text{end}}(\hbar\omega) = \sum_{s=\pm} \sum_{\lambda,\sigma} \sum_{l,m,n} C_{\alpha,l} C_{\beta,m} C_{\nu,n} \times \delta(\hbar\omega - s(E_{\lambda,\sigma}^s + lE_{\alpha} + mE_{\beta} + nE_{\nu})), \quad (16)$$

where s is the index for the positive and negative energy region, $\lambda = \pm$, $\sigma = \pm$ are the band and spin indices, the summations l, m, n run on all integers. $E_{\lambda,\sigma}^+ = \sum_j c_j E_j N_j + \lambda \varepsilon_0 \delta - eV_G$ and $E_{\lambda,\sigma}^- = E_{\text{c+}} + 3\varepsilon_0/4 - E_{\lambda,\sigma}^+$, where $c_j = 1, \lambda, \sigma, \lambda\sigma$ for $j = \text{c+}, \text{c-}, \text{s+}, \text{s-}$, respectively. When the temperature is much lower than the level spacings, $k_{\text{B}}T \ll E_{\mu}$, the coefficients $C_{\mu,p}$ are written as

$$C_{\mu,p} = C_{\mu,p}^{T=0} + \gamma_{\mu} e^{-E_{\mu}/k_{\text{B}}T} (C_{\mu,p+1}^{T=0} + C_{\mu,p-1}^{T=0} - 2C_{\mu,p}^{T=0}), \quad (17)$$

$$C_{\mu,p}^{T=0} = \frac{\Gamma(\gamma_{\mu} + p)}{p! \Gamma(\gamma_{\mu})} C_{\mu,0}^{T=0} \Theta(p). \quad (18)$$

Here Γ is the Gamma function and Θ is the step function. The coefficient γ_{μ} corresponds to the end-tunneling exponents in the bosonic correlation functions, with

$$\gamma_{\alpha} = \frac{1}{4g} \frac{E_{\alpha}}{\varepsilon_{\text{c+}}} \sin^2 \varphi, \quad \gamma_{\beta} = \frac{1}{4g} \frac{E_{\beta}}{\varepsilon_{\text{c+}}} \cos^2 \varphi, \quad (19)$$

and $\gamma_{\nu} = 3/4$. The phase φ is defined by $\varphi = \arctan(-4I\sqrt{\varepsilon_a \varepsilon_{\text{c+}}}/(\varepsilon_a^2 - \varepsilon_{\text{c+}}^2))/2$. Thus, from (16), one sees that at low temperatures a signature of the finite length of the SWNT appears in the form of discrete peaks in the density of states. More precisely, three peak families with distinct periods are identified, cf. Fig. 1, reflecting (i) the discrete excitations of the (renormalized) charge density with energy spacing

E_β , (ii) the excitations of the neutral sectors with spacing E_ν , and (iii) the phonon-assisted-like excitations with spacing E_α . At zero temperature the l -th phonon peak height with respect to that of the corresponding electron excitation peak is given by $C_{\alpha,l}^{T=0}/C_{\alpha,0}^{T=0} = \gamma_\alpha(\gamma_\alpha + 1) \cdots (\gamma_\alpha + l - 1)/l!$. For example, the ratio for $l = 1$ is simply γ_α . For large γ_μ it holds the asymptotic relation

$$C_{\mu,p}^{T=0} \simeq \frac{\gamma_\mu^p}{p!} C_{\mu,0}^{T=0} \Theta(p), \quad (20)$$

which resembles the relation among satellite peaks due to vibron-assisted tunneling as in [32]. For large p , on the other hand, each peak series shows power-law in its height, because the relation $C_{\mu,p}^{T=0} \propto p^{\gamma_\mu - 1}$ holds if one uses the asymptotic expansion for the Gamma function.

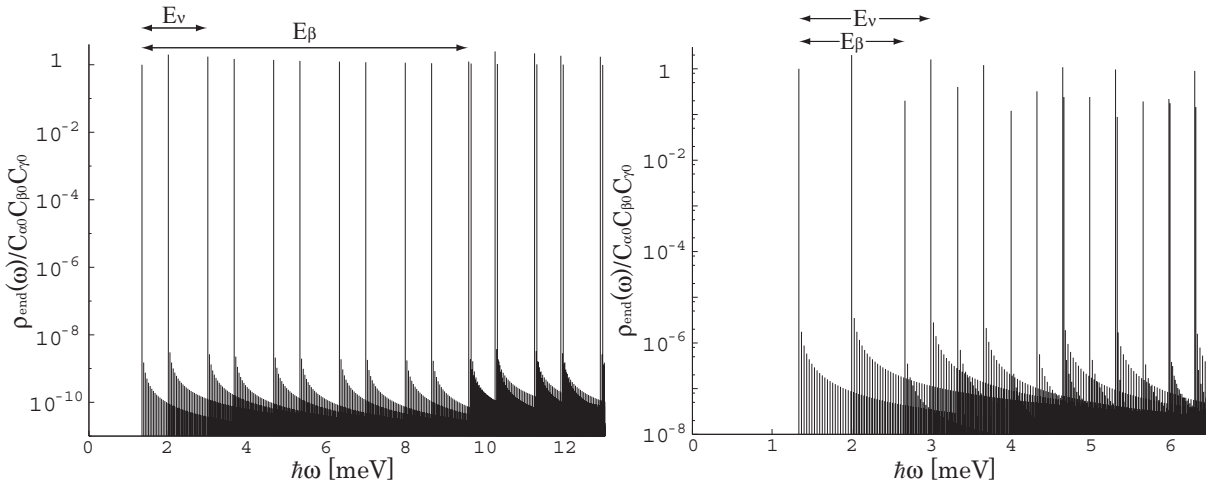


Figure 1. End-tunneling density of states of a (10,10) SWNT vs. frequency for strongly interacting electrons ($g = 0.2$, left figure) and non-interacting electrons ($g = 1$, right figure). Only the positive energy region is shown. We use the parameters $E_{++}^+ = E_{+-}^+ = 2$ meV, $E_{-+}^+ = 2.99$ meV, and $E_{--}^+ = 1.34$ meV for both figures. This parameter set corresponds to the condition $N_{c-} = -1$, $N_{s+} = 1$, $N_{s-} = -1$, and finite band off-set $\delta = 0.2$, in which there is an unpaired electron in the $\lambda = -$ band so that a spin-1/2 appears in the SWNT. The no peak region in $0 \leq \hbar\omega \leq 1.34$ is the Coulomb blockage region. The large three peaks at 1.34, 2 and 2.99 meV reflect the different addition energy to each level in the SWNT. For each of these addition energy peaks, three families of peaks are clearly identified. They are associated to the plasmon, phonon and "neutral" bosonic excitations of the suspended SWNT E_β , E_α and E_ν , respectively. Because the relation $E_{-+}^+ = E_{--}^+ + E_\nu$ holds for the present electron configuration, some of the excitation peaks stemming from $\hbar\omega = E_{-+}^+$ are degenerate with some of those stemming from $\hbar\omega = E_{--}^+$. The remaining parameters for the left figure are $E_\alpha = 0.0410$ meV, $E_\beta = 8.23$ meV, $E_\nu = 1.66$ meV, $\gamma_\alpha = 1.52 \times 10^{-9}$, $\gamma_\beta = 1.24$, $\gamma_\nu = 3/4$, $T = 0$. For the right figure, $E_\alpha = 0.0327$ meV, $E_\beta = 1.33$ meV, $E_\nu = 1.66$ meV, $\gamma_\alpha = 1.76 \times 10^{-6}$, $\gamma_\beta = 0.201$, $\gamma_\nu = 3/4$, $T = 0$.

Here we estimate the amplitudes of the phonon peaks and the excitations' spacings. First, we use the following quantities [10, 27]: $v_F = 8 \times 10^5$ m/sec, $v_{\text{st}} = 1.99 \times 10^4$ m/sec,

$c = 20\text{eV}$, $R = 6.79\text{\AA}$ (for a $(10, 10)$ armchair SWNT), $\zeta = 2\pi RM$, ($M = 3.80 \times 10^{-7}\text{kg/m}^2$), and $L = 1.0 \times 10^{-6}\text{m}$. These values give (for $g = 0.2$ then $a_B = 0.993$) the energies $E_\alpha = 0.0410\text{meV}$, $E_\beta = 8.23\text{meV}$, $E_\nu = 1.66\text{meV}$, $\gamma_\alpha = 1.52 \times 10^{-9}$, and $\gamma_\beta = 1.24$, The estimated peak ratio γ_α is quite small. However, we note that the value is sensitive to the parameters. We may have $g \sim 1$ for the screening caused by the gate electrode. For $g = 1$ ($a_B = 0.804$), $E_\alpha = 0.0327\text{meV}$, $E_\beta = 1.33\text{meV}$, $E_\nu = 1.66\text{meV}$, $\gamma_\alpha = 1.76 \times 10^{-6}$, and $\gamma_\beta = 0.201$. The sensitivity of γ_α will be discussed in the next paragraph. We also note that there is an uncertainty in the precise value of the coupling constant c . Estimates in [27] yield values $c \simeq 14 - 21\text{eV}$.

In Fig. 2, the ratio of the first phonon peak height γ_α as a function of the charge plasmon energy spacing and of the electron-phonon coupling is plotted. For very strong

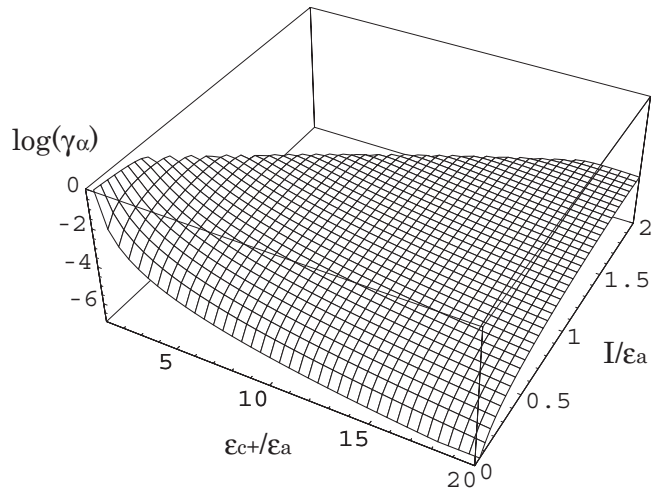


Figure 2. Relative phonon peak height γ_α as a function of the ratio between charge-plasmon and longitudinal phonons level spacing $\varepsilon_{c+}/\varepsilon_a$, and of the electron-phonon coupling I/ε_a . The vertical axis is in logarithmic scale. The back side region without mesh is the WB singularity region, where γ_α has an imaginary value.

couplings, corresponding to the condition $I^2 > \varepsilon_a \varepsilon_{c+}/4$, the system becomes unstable, as the Wenztel-Bardeen (WB) singularity is approached. In general the ratio is very sensitive to the parameters. The peak height becomes larger for small charge velocities, especially close to the WB singularity. For the small coupling case, the system survives the collapse for a wide range of parameters while the charge velocity is increased, until finally the approach of the singularity is expected.

4. Conclusion

From our semi-quantitative discussion, it follows that the phonon peaks could be observed in experiments. In recent experiments [33] on suspended metallic carbon nanotubes, many excitation peaks have been observed in the differential conductance. The peaks appear outside of the Coulomb diamonds, and are almost equidistantly

spaced. The period of the peaks is about 0.53meV for a $L = 140\text{nm}$ length nanotube, 0.69meV for a $L = 420\text{nm}$, and 0.14meV for a $L = 1200\text{nm}$, respectively. The theoretical estimate of the period for the phonon assisted peaks is 0.77 to 0.09meV, while that for the charge density is 47.5 to 5.5meV (if $g \sim 0.2$), and 9.5 to 1.1meV for the neutral sectors. The observed peaks might be the phonon-assisted peaks discussed in this paper. The relative peak height γ_α reflects the strength of the electron-phonon coupling. From the experimental data in Ref. [33] a rough estimate $\gamma_\alpha \sim 0.3$ to 0.8 can be extracted. These values are much larger than those we estimated in the previous section for strong Coulomb interaction ($g \sim 0.2$). Moreover, the experiments seem to well agree with the asymptotic formula (20). This could be an indication of a strong renormalization of the electronic parameters expected when the system is close to the WB singularity. Thus, while a qualitative agreement with the experiments is found, an understanding of the lack of a quantitative agreement clearly calls for further theoretical investigations. We mention that a relation similar to (20) has also been predicted for electronic degrees of freedom dressed by a Frank-Condon factor originating from a generic vibron-electron coupling. However, also the theoretical expectation for the values of the coupling in the model in [32] seems to be much smaller than the one extracted from experiments [33].

For temperatures larger than the level spacing finite size effects are washed out, and we can adapt our calculation to the case of a SWNT of infinite length. The density of states for this case becomes:

$$\rho_{\text{end}}(\hbar\omega) \sim |\omega|^{\frac{1}{4}(\frac{1}{g'}+3)-1}, \quad (21)$$

where g' is the interaction parameter renormalized by the electron-phonon interaction, $(g')^{-1} = 4(\gamma_\alpha + \gamma_\beta)$. As expected, the charge, neutral and phonon peaks are washed out and the density of states shows a simple power-law behavior with exponent modified by the electron-phonon interaction. The renormalized parameter g' is always larger than g , showing that the phonons contribute to an effective *attractive* electron-electron interaction.

When a gate voltage is applied to the nanotube, the possibility to investigate Coulomb blockade phenomena and Kondo-correlation effects arises. In the presence of a gate potential the coupling between the electrons and the transverse bending mode should be included. One can control the coupling strength by changing the gate potential. Because the bending phonon mode couples to many of the charge density modes, and it has less energy for the vibration, an instability might be easily induced. The effects of the gate potential will be discussed elsewhere.

In conclusion, we have discussed transport properties of a suspended metallic SWNT. The low energy excitations caused by the stretching phonons are expected to appear as small periodic peaks beside the peaks for the charged and neutral electronic-like modes in the differential conductance. Each series of peaks exhibit a different power-law. When the system is close to the WB singularity, the phonon peaks are large enough in height to be observed. The observation of the phonon peaks would thus indicate that the singularity is approached.

Acknowledgments

We thank S. Sapmaz, Y. M. Blanter, L. Mayrhofer, R. Saito for valuable discussions. This work was supported by the Fundamental Research on Matter in the Netherlands; by the Grant-in-Aid No. 16740166 from the Ministry of Education, Culture, Sport, Science and Technology, of Japan; by the Deutsche Forschungsgemeinschaft (GRK 638).

Appendix: Density of states of suspended SWNTs

Here we show the detailed calculation of the density of states at the end of a finite length nanotube. Let us consider a high enough tunneling barrier between electrodes and the nanotube. At low temperature, the differential conductance is proportional to the density of states at the end of the nanotube

$$dI/dV_{\text{bias}} \propto \rho_{\text{end}}(\hbar\omega = eV_{\text{bias}}) = -\text{Im}G_{\text{end}}(\hbar\omega = eV_{\text{bias}})/\pi, \quad (22)$$

where $G_{\text{end}}(\hbar\omega) \equiv G(x, x'; \hbar\omega)|_{x=x' \rightarrow \xi}$ is the Fourier transform of the retarded Green's function $G(x, x'; t) = \frac{1}{i\hbar}\Theta(t)\langle\Psi(x, t)\Psi^\dagger(x', 0) + \Psi^\dagger(x', 0)\Psi(x, t)\rangle$, and ξ is a length which is of the order of the inverse of the Fermi wave length. The electron field operator is written in terms of boson operators using the bosonization identity [34]

$$\Psi_\eta(x, t) = \frac{1}{\sqrt{2\pi\epsilon}}U_\eta e^{i\kappa_\eta x}e^{-\frac{i}{2}\sum_j c_j \theta_{j,r}(x, t)}, \quad (23)$$

and $\Psi(x, t) = \sum_\eta \Psi_\eta(x, t)$. Here $\eta = (r, \lambda, \sigma)$ is the parameter set of the left and right going wave ($r = -, +$), the band index of the nanotube ($\lambda = \pm$), and the spin index ($\sigma = \pm$). $\epsilon \rightarrow 0$ is the cut-off length, U_η is the Klein factor, $\kappa_\eta = r\lambda k_F + r(N_\eta + \lambda\delta)\pi/L$ and N_η is the number of electrons in the η -branch. $k_F = 2\pi/3a$ is the Fermi wave length, a is the honeycomb lattice constant, and we consider the case $k_F \gg |N_\eta|\pi/L$ in this paper to justify our low-energy theory. The field $\theta_{j,r}$ is written as,

$$\theta_{j,r}(x, t) = \sqrt{\frac{\pi}{\hbar}} \left(-r\phi_j(x, t) + \int^x dx' \Pi_j(x') \right). \quad (24)$$

We note that the left and right going waves are not independent anymore in the case of open boundary condition; the relation $\Psi_{r,\lambda,\sigma}(x) = -\Psi_{-r,\lambda,\sigma}(-x)$ holds.

Let us consider the correlation function in the Green's function $\langle\Psi(x, t)\Psi^\dagger(x', 0)\rangle$. This can be separated into the boson and the fermion parts;

$$\begin{aligned} \langle\Psi(x, t)\Psi^\dagger(x', 0)\rangle &= \sum_\eta \frac{1}{2\pi\epsilon} \langle U_\eta(t)U_\eta^\dagger(0) \rangle \\ &\times \left\{ e^{i\kappa_\eta(x-x')} \Pi_j \langle e^{-i\frac{1}{2}c_j \theta_{j,r}(x, t)} e^{i\frac{1}{2}c_j \theta_{j,r}(x', 0)} \rangle \right. \\ &\quad \left. - e^{i\kappa_\eta(x+x')} \Pi_j \langle e^{-i\frac{1}{2}c_j \theta_{j,r}(x, t)} e^{i\frac{1}{2}c_j \theta_{j,r}(-x', 0)} \rangle \right\}. \end{aligned} \quad (25)$$

Since the Klein factor only changes the number of electrons in η -branch, the fermion part of the correlation function can be calculated as, $\langle U_\eta(t)U_\eta^\dagger(0) \rangle = \exp(-i\frac{E_{N_\eta+1} - E_{N_\eta}}{\hbar}t)$. Here $E_{N_\eta+1} - E_{N_\eta} = E_{\lambda,\sigma}^+$ being addition energies of the η -branch. (Because of the open boundary condition, we have no r dependence in the addition energies). On the

other hand, using the relation for bosonic operators, $\langle e^{-iA}e^{iB} \rangle = e^{-\frac{1}{2}\langle A^2 \rangle - \frac{1}{2}\langle B^2 \rangle + \langle AB \rangle}$, the bosonic part of the correlation function can be written as

$$\begin{aligned} & \langle e^{-\frac{i}{2}c_j\theta_{j,r}(x,t)}e^{\frac{i}{2}c_j\theta_{j,r}(x',0)} \rangle \\ &= e^{\{-\frac{1}{2}\langle \theta_{j,r}^2(x,t) \rangle - \frac{1}{2}\langle \theta_{j,r}^2(x',0) \rangle + \langle \theta_{j,r}(x,t)\theta_{j,r}(x',0) \rangle\}/4}, \end{aligned} \quad (26)$$

which doesn't depend on λ, σ . Therefore the calculation can be reduced to that for the bosonic correlation function, $\langle \theta_{j,r}(x,t)\theta_{j,r}(x',0) \rangle$. Now we discuss the correlation function of the charge sector. Similar calculations have been done for the neutral sectors. Substituting the Eqs. (6), (7) into (24), and using the Bogoliubov transformation

$$\begin{pmatrix} \beta_n^\dagger \\ \beta_n \\ \alpha_n^\dagger \\ \alpha_n \end{pmatrix} = \hat{A}_n \hat{B}_n \hat{C}_n \begin{pmatrix} b_{c+,n}^\dagger \\ b_{c+,n} \\ a_n^\dagger \\ a_n \end{pmatrix}, \quad (27)$$

where

$$\hat{A}_n = \begin{pmatrix} \frac{1}{\sqrt{E_\beta n}} & -i\sqrt{E_\beta n} & 0 & 0 \\ \frac{1}{\sqrt{E_\beta n}} & i\sqrt{E_\beta n} & 0 & 0 \\ 0 & 0 & \sqrt{E_\alpha n} & -\frac{i}{\sqrt{E_\alpha n}} \\ 0 & 0 & \sqrt{E_\alpha n} & \frac{i}{\sqrt{E_\alpha n}} \end{pmatrix}, \quad (28)$$

$$\hat{B}_n = \begin{pmatrix} \cos \varphi & 0 & 0 & -\sin \varphi \\ 0 & \cos \varphi & \sin \varphi & 0 \\ 0 & -\sin \varphi & \cos \varphi & 0 \\ \sin \varphi & 0 & 0 & \cos \varphi \end{pmatrix}, \quad (29)$$

$$\hat{C}_n = \begin{pmatrix} \frac{i}{2}\sqrt{\varepsilon_{c+}n} & -\frac{i}{2}\sqrt{\varepsilon_{c+}n} & 0 & 0 \\ -\frac{1}{2\sqrt{\varepsilon_{c+}n}} & -\frac{1}{2\sqrt{\varepsilon_{c+}n}} & 0 & 0 \\ 0 & 0 & \frac{1}{2\sqrt{\varepsilon_a n}} & \frac{1}{2\sqrt{\varepsilon_a n}} \\ 0 & 0 & \frac{i}{2}\sqrt{\varepsilon_a n} & -\frac{i}{2}\sqrt{\varepsilon_a n} \end{pmatrix}, \quad (30)$$

(31)

at the end of nanotube $x = x' \rightarrow \xi$, the correlation function satisfies the relation

$$\begin{aligned} & \langle \theta_{c+,r}(x,t)\theta_{c+,r}(x',0) \rangle \\ &= \frac{1}{g_j} \frac{\pi}{L} \sum_{n \geq 1} \frac{1}{k_n} \left\{ \frac{E_\beta}{\varepsilon_{c+}} \cos^2 \varphi \langle \beta_n(t)\beta_n^\dagger(0) + \beta_n^\dagger(t)\beta_n(0) \rangle \right. \\ & \quad \left. + \frac{E_\alpha}{\varepsilon_{c+}} \sin^2 \varphi \langle \alpha_n(t)\alpha_n^\dagger(0) + \alpha_n^\dagger(t)\alpha_n(0) \rangle \right\}, \end{aligned} \quad (32)$$

which doesn't depend on r . The lowest order of the function with respect to ξ is $O(\xi^0)$, therefore we calculate the bosonic correlation function at $x = x' = 0$ hereafter. Using the relation

$$\langle \beta_n(t)\beta_n^\dagger(0) + \beta_n^\dagger(t)\beta_n(0) \rangle = \cos(E_\beta n t) \cosh\left(\frac{E_\beta n}{2k_B T}\right) - i \sin(E_\beta n t), \quad (33)$$

and multiplying by $e^{-\hbar v k_n / E_{\text{cut}}}$ each term of the summation over n in Eq. (32) to avoid divergences in the calculation, where $E_{\text{cut}} = \hbar v \epsilon^{-1} (\rightarrow \infty)$ is a cut-off energy and $v = E_{\alpha/\beta} L / \pi \hbar$, then the exponent of the Green's function is written as

$$\begin{aligned} & \langle \theta_{j,r}^2(0, t) \rangle + \langle \theta_{j,r}(0, t) \theta_{j,r}(0, 0) \rangle \\ &= - \frac{1}{g_{c+}} \frac{E_\beta}{\epsilon_{c+}} \cos^2 \varphi \left\{ \log \frac{1 - e^{-E_\beta/E_{\text{cut}}} e^{-iE_\beta t/\hbar}}{e^{-E_\beta/E_{\text{cut}}}} \right. \\ & \quad \left. + \sum_m \log \frac{\cosh(\frac{E_\beta}{E_{\text{cut}}} + \frac{mE_\beta}{k_B T}) - \cos(\frac{E_\beta}{\hbar} t)}{\cosh(\frac{E_\beta}{E_{\text{cut}}} + \frac{mE_\beta}{k_B T}) - 1} \right\} \\ & \quad + \{\beta \rightarrow \alpha, \cos \varphi \rightarrow \sin \varphi\}, \end{aligned} \quad (34)$$

where we use the identities

$$\cosh x = 1 + 2 \sum_{n=1}^{\infty} e^{-2nx}, \quad (35)$$

$$\sum_{n=1}^{\infty} \frac{e^{-nx}}{n} = -\log(1 - e^{-x}). \quad (36)$$

Then the boson part of the correlation function is calculated as

$$\langle e^{-\frac{i}{2}\theta_{j,r}(0,t)} e^{\frac{i}{2}\theta_{j,r}(0,0)} \rangle = D_\alpha(t) D_\beta(t), \quad (37)$$

where, up to orders $(\exp\{-E_\beta/k_B T\})$,

$$\begin{aligned} D_\beta(t) &= \left(\frac{1 - e^{-E_\beta/E_{\text{cut}}} e^{-iE_\beta t/\hbar}}{e^{-E_\beta/E_{\text{cut}}}} \right)^{-\gamma_\beta} \\ & \quad \times \prod_m \left(\frac{\cosh(\frac{E_\beta}{E_{\text{cut}}} + \frac{mE_\beta}{k_B T}) - \cos(\frac{E_\beta}{\hbar} t)}{\cosh(\frac{E_\beta}{E_{\text{cut}}} + \frac{mE_\beta}{k_B T}) - 1} \right)^{-\gamma_\beta} \end{aligned} \quad (38)$$

$$= \sum_{p=-\infty}^{\infty} D_{\beta,p} e^{-ip\frac{E_\beta}{\hbar}t}, \quad (39)$$

where

$$D_{\beta,p} = D_{\beta,p}^{T=0} + \gamma_\beta e^{-E_\beta/k_B T} (D_{\beta,p+1}^{T=0} + D_{\beta,p-1}^{T=0} - 2D_{\beta,p}^{T=0}), \quad (40)$$

$$D_{\beta,p}^{T=0} = \frac{(1 - e^{-E_\beta/E_{\text{cut}}})^{\gamma_\beta}}{E_\beta/\hbar} e^{-pE_\beta/E_{\text{cut}}} \frac{\Gamma(\gamma_\beta + p)}{p! \Gamma(\gamma_\beta)} \Theta(p), \quad (41)$$

and $\beta \rightarrow \alpha$ for $D_\alpha(t)$. After a similar calculation for the neutral sectors and for $\langle \Psi^\dagger(x', 0) \Psi(x, t) \rangle$, we finally get the Green's function

$$\begin{aligned} G_{\text{end}}(\hbar\omega) &= \frac{2 \sin^2(k_F \xi)}{\pi \epsilon} \sum_{s=\pm} \sum_{\lambda, \sigma} \sum_{l, m, n} D_{\alpha,l} D_{\beta,m} D_{\nu,n} \\ & \quad \times \frac{1}{\hbar\omega - s(E_{\lambda, \sigma}^s + lE_\alpha + mE_\beta + nE_\nu) + i0_+}. \end{aligned} \quad (42)$$

After re-definition of the coefficients, e.g., $C_{\mu,p} = D_{\mu,p} (2 \sin^2(k_F \xi) / \pi \epsilon)^{1/3}$, we get the density of states (16).

References

- [1] For example, see, R. Saito, G. Dresselhaus and M. S. Dresselhaus, *Physical Properties of Carbon Nanotubes*, Imperial College Press, London, 1998.
- [2] J. W. G. Wildöer, L. C. Venema, A. G. Rinzler, R. E. Smalley and C. Deller, *Nature* **391**, 59 (1998).
- [3] T. W. Odom, J. L. Huang, P. Kim and C. M. Lieber, *Nature* **391**, 62 (1998).
- [4] S. J. Tans, M. H. Devoret, H. Dai, A. Thess, R. E. Smalley, L. J. Geerligs and C. Dekker, *Nature* **386**, 474 (1997).
- [5] M. Bockrath, D. H. Cobden, P. L. McEuen, N. G. Chopra, A. Zettl, A. Thess, R. E. Smalley, *Science* **275**, 1922 (1997).
- [6] J. Nygård, D. H. Cobden and P. E. Lindelof, *Nature* **408**, 342 (2000).
- [7] M. Bockrath, D. H. Cobden, J. Lu, A. G. Rinzler, R. E. Smalley, L. Balents and P. L. McEuen, *Nature* **397**, 598 (1999).
- [8] J. Nygård, D. H. Cobden, M. Bockrath, P. L. McEuen and P. E. Lindelof, *Appl. Phys. A* **69**, 297 (1999).
- [9] R. Egger and A. O. Gogolin, *Phys. Rev. Lett.* **79**, 5082 (1997).
- [10] C. Kane, L. Balents and M. P. A. Fisher, *Phys. Rev. Lett.* **79**, 5086 (1997).
- [11] R. Egger and A. O. Gogolin, *Eur. Phys. J. B* **3**, 281 (1998).
- [12] J. Nygård and D. H. Cobden, *Appl. Phys. Lett.* **79**, 4216 (2001).
- [13] N. R. Franklin, Q. Wang, T. W. Tombler, A. Javey, M. Shim and H. Dai, *Appl. Phys. Lett.* **81**, 913 (2002).
- [14] P. Jarillo-Herrero, S. Sapmaz, C. Dekker, L. P. Kouwenhoven and H. S. J. van der Zant, *Nature* **429**, 389 (2004).
- [15] V. Sazonova, Y. Yaish, H. Üstünel, D. Roundy, T. A. Arias and P. L. McEuen, *Nature* **431**, 284 (2004).
- [16] B. J. LeRoy, S. G. Lemay, J. Kong and C. Dekker, *Nature* **432**, 371 (2004).
- [17] B. Babic, J. Furer, S. Sahoo, Sh. Fahrangfar and C. Schönenberger, *Nanolett.* **3**, 1577 (2003).
- [18] A. Komnik and A. O. Gogolin, *Phys. Rev. B* **66**, 125106 (2002).
- [19] S. Sapmaz, Y. M. Blanter, L. Gurevich and H. S. J. van der Zant, *Phys. Rev. B* **67**, 235414 (2003).
- [20] A. De Martino and R. Egger, *Phys. Rev. B* **67**, 235418 (2003).
- [21] Y. M. Blanter, O. Usmani and Y. N. Nazarov, *Phys. Rev. Lett.* **93**, 136802 (2004).
- [22] F. D. M. Haldane, *J. Phys. C: Solid State Phys.*, **14**, 2585 (1980).
- [23] S. Sapmaz, P. Jarillo-Herrero, J. Kong, C. Dekker, L.P. Kouwenhoven and H.S.J. van der Zant, *Phys. Rev. B* **71**, 153402 (2005).
- [24] M. Ouyang, J.-L. Huang, C. L. Cheung, C. M. Lieber, *Science* **292**, 702 (2001).
- [25] M. Fabrizio and A. O. Gogolin, *Phys. Rev. B* **51**, 17827 (1995).
- [26] A. E. Mattsson, S. Eggert and H. Johannesson, *Phys. Rev. B* **56**, 15615 (1997).
- [27] H. Suzuura and T. Ando, *Phys. Rev. B* **65**, 235412 (2002).
- [28] D. Loss and T. Martin, *Phys. Rev. B* **50**, 12160 (1994).
- [29] H. J. Schulz, *Phys. Rev. Lett.* **64**, 2831 (1990).
- [30] M. Fabrizio, C. Castellani and C. Di Castro, *Int. J. Mod. Phys. B* **10**, 1439 (1996).
- [31] P. Kleinert and V. V. Bryksin, *Phys. Stat. Sol. B* **199**, 435 (1997).
- [32] S. Braig and K. Flensberg, *Phys. Rev. B* **68**, 205324 (2003).
- [33] S. Sapmaz, P. Jarillo-Herrero, Y. M. Blanter, C. Dekker and H. S. J. van der Zant, *cond-mat/0508270*.
- [34] In this derivation we neglect a slowly oscillating prefactor which comes by considering the three-dimensional nature of the nanotube wavefunctions. See e.g. Ref. [9].